International Journal of Mass Spectrometry 289 (2010) 119–127

Contents lists available at ScienceDirect

International Journal of Mass Spectrometry

journal homepage: www.elsevier.com/locate/ijms

Protein isolation through impact desolvation of electrosprayed microdroplets (IDEM): Molecular dynamics simulation

Saravana Prakash Thirumuruganandham, Herbert M. Urbassek*

Fachbereich Physik und Forschungszentrum OPTIMAS, Universität Kaiserslautern, Erwin-Schrödinger-Straße, D-67663 Kaiserslautern, Germany

ARTICLE INFO

Article history:
Received 11 August 2009
Received in revised form
24 September 2009
Accepted 1 October 2009
Available online 9 October 2009

PACS:
79.20.Ap
82.80.Ms
87.15.ap
87.15.kr
87.15.hp

Keywords:
Molecular dynamics
Mass spectrometry
Protein–solvent interaction
Conformational change
Impact desolvation

ABSTRACT

Using molecular dynamics simulation, we investigate the collision of an echistatin molecule embedded in a 3330 molecule water droplet with a repulsive wall, such as it is relevant in the *impact desolvation of electrosprayed microdroplets* (IDEM) process. Protein denaturation and conformation stability are studied by monitoring the time evolution of the radius of gyration, the root mean squared deviation of the protein backbone, the solvent accessible and excluding surface areas, the secondary structure and by an analysis of the hydrogen bond network. The resulting dehydration process of the protein occurs on a time scale spanning at least tens of ps, and depends sensitively on the collision speed. We find that at the lowest impact velocities of 1.6–2.9 km/s the protein remains covered by a water shell and exhibits only little distortions. At the highest impact velocities (3.7–4.1 km/s) the protein is entirely dehydrated and strongly distorted. The minimum thickness of the hydration shell which is needed to preserve the non-denatured conformation of the protein, one monolayer of water, can be obtained by carefully tuning the impact velocity.
© 2009 Elsevier B.V. All rights reserved.

1. Introduction

The *impact desolvation of electrosprayed microdroplets* (IDEM) technique is one of several biomolecular mass spectrometry methods, which have the aim of obtaining an intact solvent-free biomolecule in the gas phase ready for mass spectrometry. In the IDEM process, sample molecules are dissolved in an electrolyte solution which is fed through a capillary and electrosprayed in vacuum, producing highly charged, analyte-containing microdroplets that are accelerated in an electric field and impacted on an inert target with velocities of several km/s. The kinetic energy has to be chosen such that it is sufficient to fully desolvate the biomolecular ions following impact on the target surface without fragmenting them [1]. The desolvation process of IDEM is broadly tunable by varying the impact energy of the droplet. Initial experiments were performed on oligonucleotides and peptides (bradykinin, neurotensin); these samples yielded singly and doubly charged molecular ions with no detectable fragmentation [1].

The IDEM method is related to the earlier method known as massive cluster impact (MCI), introduced in 1991 by Mahoney et al. [2]. In MCI, large, highly charged electrosprayed liquid clusters are accelerated in vacuum to velocities of several km/s and used as projectiles to desorb biomolecular ions from the surface of a solid or liquid target. For vacuum compatibility, MCI requires either dried targets or samples dissolved in involatile solvents such as liquid glycerol. Therefore, it cannot sample ions directly from the aqueous solutions which are most often encountered in biochemical analysis. In contrast, IDEM allows direct sampling of biomolecular analytes from aqueous solutions.

Recent research studies have been conducted to understand the fundamental mechanisms associated with cluster–surface and droplet–surface interactions. In the field of cluster impact chemistry, molecular dynamics has been used to study the fragmentation behaviour of clusters of $(NH_3)_nH^+$ as well as mixed species of I_2Ar_n and $(CH_3I)_n^-$ at different impact velocities onto a wall [3–5]. Recent molecular dynamics investigations of N_2 cluster impact onto a rigid wall describe the complete fragmentation, molecule dissociation and intact reflection regimes [6,7]. In addition to cluster–wall interaction studies, the related field of cluster–cluster interaction has received vivid interest. Wyatt presented results from molecular dynamics simulations of binary collisions of $(H_2O)_{400}$ droplets

* Corresponding author.
E-mail address: urbassek@rhrk.uni-kl.de (H.M. Urbassek).
URL: http://www.physik.uni-kl.de/urbassek/ (H.M. Urbassek).

1387-3806/$ – see front matter © 2009 Elsevier B.V. All rights reserved.
doi:10.1016/j.ijms.2009.10.002

featuring the coalescence, stretching separation, and scattering phenomena [8]. Svanberg et al. employed $(H_2O)_{125}$ and $(H_2O)_{1000}$ clusters and performed simulations for two different initial temperatures of 160 and 300 K to explain the boundary between coalescence and stretching separation of water droplets [9]. These atomistic studies supplement earlier fluid dynamics studies of the coalescence of liquid droplets as well as their deformation and breakup in viscous flows [10,11].

In the field of biomolecular mass spectrometry, computational studies have been conducted for understanding the protein structure and stability in different mass spectrometric techniques such as electrospray ionization (ESI), matrix-assisted laser desorption (MALDI), MCI, laser spray, and laser-induced liquid beam ionization (LILBID) [12–16]. Electrospray ionization is a common method to transfer large biomolecular ions from solution to the gas phase [17]. The role of jets and filaments in the electrospray process has been extensively investigated on the macroscopic scale [18–20]. For example, recent results of acidic and basic aqueous solutions of α-lactalbumin in positive and negative mode operations has found no remarkable differences in the laser and electro spray process [21]. On the other hand, denaturation was found at positive mode operation for ubiquitin. In contrast, for both α-lactalbumin and ubiquitin laser-induced denaturation was not observed for the negative mode operations of laser spray as well as electro spray [21].

Atomistic simulations have been able to explain several important aspects of biomolecular mass spectrometry. It was noticed that in the ESI process, large non-covalent complexes like the chaperonin GroEL can be transferred into the gas phase intact [22]. Mao et al. [23] have studied the effect of ion net charge on the compactness, stability and hydration of unsolvated cytochrome *c* ions using molecular dynamics simulations. Previous studies of hydration levels of myoglobin by molecular dynamics suggest that, to conserve the native structure of the protein, a moderate water coverage of ∼ 350 water molecules for myoglobin is needed [24]. These gentle ionization methods permit studies of unsolvated biomolecules [25]. Furthermore, solvent molecules can be added one at a time so that properties can be investigated as a function of the degree of solvation. Studies of unsolvated peptides and proteins are of interest for more than just fundamental reasons [25]. A study of the desolvation process allows to understand the behaviour of protein structure in different mass spectrometry setups. Aqueous solution is not the only biologically important environment, membrane proteins make up to 30% of the proteins encoded by genomes, and the hydrophobic and low dielectric interior of a lipid bilayer is very different from an aqueous environment. The hydrophobic interior of folded proteins is also largely shielded from solvent interactions. Studies of the intramolecular interactions in the absence of the solvent can help to understand the solvent-depleted regions [25], with respect to protein in water and gas phase and its significance in mass spectrometry studies.

In this paper we investigate the IDEM process at different impact energies using CHARMM molecular dynamics. An echistatin protein solvated in a water droplet is used as a model system. We examine the effects of impact energy on the desolvation, conformation and structural properties of the protein. The optimum energy to obtain solvent-free intact protein is discussed.

2. Method

For modelling the IDEM process of a biomolecular system, we have used version c31b of the CHARMM molecular dynamics software tool [26]. The empirical potential energy function adopted in CHARMM to model macromolecular systems consists of the bond stretching, bending, improper dihedral, dihedral, van der Waals, and electrostatic terms. This force field does not allow for the breaking of covalent bonds in the protein. All H bonds are kept rigid, since the corresponding vibrational frequencies are so high that they will not be excited. This approach is analogous to that used previously in MALDI studies [28,27]. To this potential, we add a planar, purely repulsive wall at $x = 0$. It is realized by an exponential potential, which acts on all atoms,

$$V_{\text{wall}}(x) = \sum_{i=1}^{N} h e^{-x_i/\lambda}, \tag{1}$$

where x_i is the distance of atom i from the wall. The strength h of the potential and its range λ are taken from the built-in potential function used in the CHARMM package to model membrane bilayer systems [1]. Water is described using the TIP3P potential [29]. In it, the O–H distance is kept rigid. We note that this approximation becomes less reliable at higher impact energies.

We employ a Verlet integrator scheme to calculate the dynamics with a time step of $\Delta t = 0.1$ fs. The SHAKE algorithm [30] is used for all hydrogen atoms. The system configuration is stored every 0.1 ps over a total simulation time of 150 ps. We employ a 14 Å cutoff for non-bonding options with a switch truncation function on both the van der Waals and the electrostatic interactions. Switching functions terminate the interaction at 12 Å, where a 2 Å switching region was employed.

To reduce the complexity of the molecular dynamics simulations of the IDEM process, we consider the structure and conformational dynamics of a small 49 amino acid residue protein, echistatin (a snake toxin), molecular weight of 5418 Da immersed in a sphere of 30 Å TIP3P water. The resulting molecular system consists of 10,703 atoms (3330 water molecules, plus 713 echistatin atoms). We study here a neutral droplet. The simulation of a charged water cluster containing a protein ion would have to be based on a modified force field.

Before starting the impact process, the protein–water droplet is carefully equilibrated in several simulation steps, since the protein and water originate from two different environments before starting the simulation. First, in order to remove bad nonbonding contacts in the protein–water complex, the system is subjected to steepest descent energy minimization for 500 molecular dynamics steps. For the heating process, the system is subjected to stochastic dynamics: while for an inner region of 0–25 Å conventional molecular dynamics is used, we apply Langevin dynamics to the outer buffer region of 25–30 Å; this procedure helps to prevent water evaporation and to conserve the spherical shape of the cluster. Then the temperature is slowly increased within 10 ps to the final temperature of 300 K.

At this time, our simulation starts; we set $t = 0$. Before starting the impact, we let the system equilibrate for a period of time of 20 ps. During this time a spherical boundary potential of 30 Å radius was used to equilibrate the protein-water system. At $t = 20$ ps, we remove the boundary potential and start the IDEM process by giving each atom the same velocity v in normal direction to the wall (in the $-x$ direction). 7 impact events were studied; the impact velocities v were evenly spaced between 1636 and 4091 m/s. The velocities v, total droplet energies E, and the impact energies per water molecule E_{H_2O} are given in Table 1.

3. Results

3.1. Temperature and evaporation

Fig. 1 gives a visual impression of the time evolution of the water droplet during and after collision with the wall for the smallest impact energy. During impact, the cluster deforms and loses water molecules sideways; this phenomenon is well known and has been termed *lateral jetting* [6,7]. Already at this stage,

Table 1
RMSD, radius of gyration, R_{gyr}, and solvent accessible/excluding surface areas of the protein echistatin for the impact events with velocity v (total droplet energy E, energy per water molecule E_{H_2O}) are calculated from the average over the last 120 ps in the simulation. Additionally, the number of hydrogen bonds within the protein (HB_{pp}) and between the protein and the water molecules (HB_{ps}) have been determined for the same period of time. The first line gives the averaged equilibrium values for an echistatin protein in bulk water at 300 K, such as they were valid before impact ($0 < t < 20$ ps).

v (m/s)	E (eV)	E_{H_2O} (eV)	RMSD (Å)	R_{gyr} (Å)	SASA (nm^2)	SESA (nm^2)	HB_{pp}	HB_{ps}
300 K			0.77	11.24	40.03	8.80	193.2	200.8
1636	908	0.25	2.63	11.15	39.64	9.54	196.3	175.6
2045	1418	0.39	5.35	11.54	42.32	7.24	221.4	160.9
2455	2042	0.56	4.34	11.48	39.53	9.57	238.5	142.8
2864	2780	0.77	4.88	12.37	36.90	10.88	305.7	85.90
3273	3631	1.00	6.21	12.19	37.37	9.45	370.1	9.14
3682	4595	1.27	6.47	10.79	35.68	12.16	335.6	0.37
4091	5673	1.56	7.33	10.71	36.81	11.69	331.7	0.00

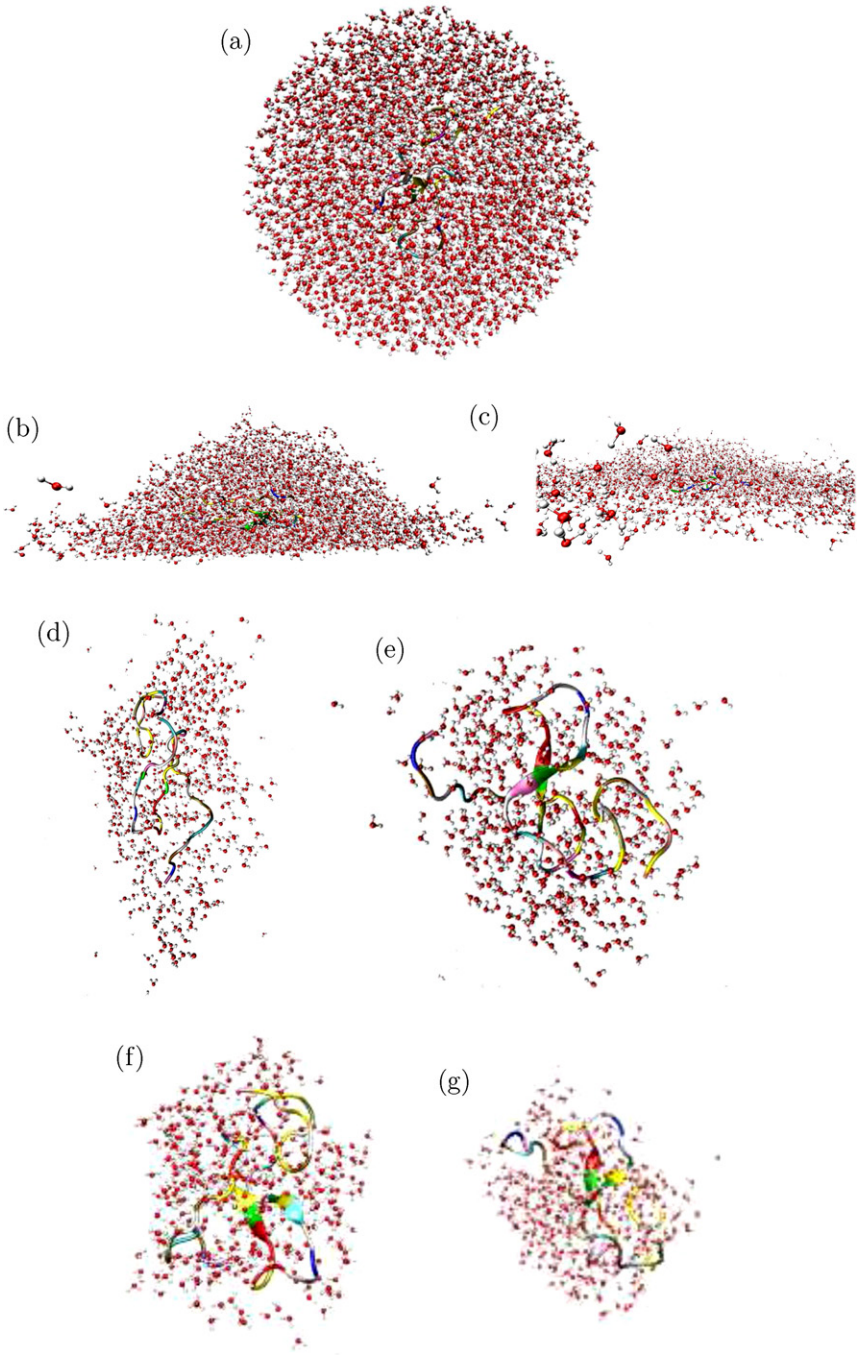

Fig. 1. Perspective snapshots of the IDEM process at an impact energy of 908 eV. (a) Before impact. (b) During impact, at time $t = 25$ ps, (c) 30 ps, (d) 70 ps, (e) 90 ps, (f) 120 ps and (g) 150 ps.

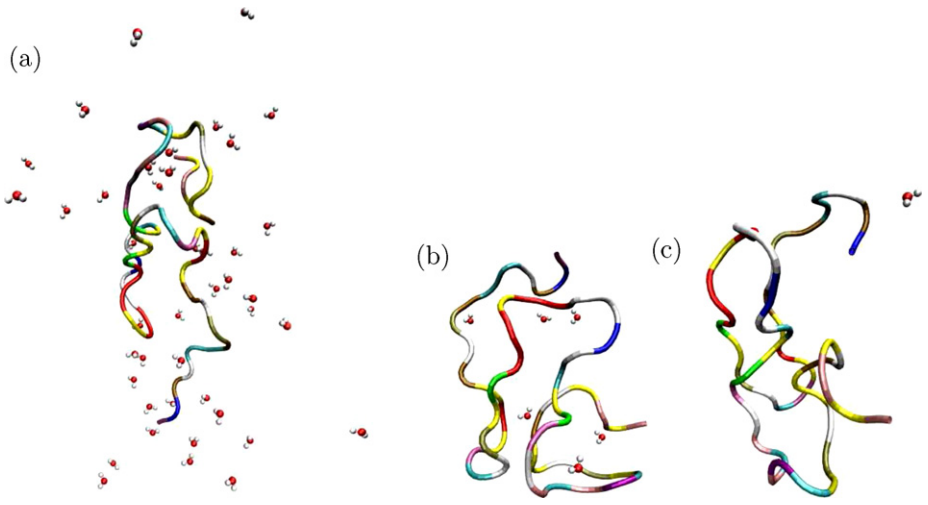

Fig. 2. Perspective snapshots of the IDEM process at an impact energy of 5673 eV. See also Supplementary Video. (a) At time $t = 31$ ps, (b) 37 ps and (c) 41 ps.

but continuing to later times, the droplet loses the majority of its water content; the protein is strongly deformed and loses its natural conformation. In the latest snapshot, water continues evaporating from the surface of the 'droplet', while the protein is still covered by its hydration shell. Fig. 2 shows a few snapshots of the desolvation process at the highest impact energy. Desolvation is seen to proceed very fast; after around 10–15 ps after impact, the protein is entirely free of water. We also observe that it is highly vibrationally excited, changing conformation very quickly.

When after $t = 20$ ps the droplet starts moving towards the wall, it needs some time until it interacts with it. Fig. 3 displays the temperature profiles of the water and of the protein in the relevant time window when the collision happens. Note that with increasing impact energy the collision occurs earlier. The protein is heated later than the water system; this is particularly clearly seen for the highest impact energies.

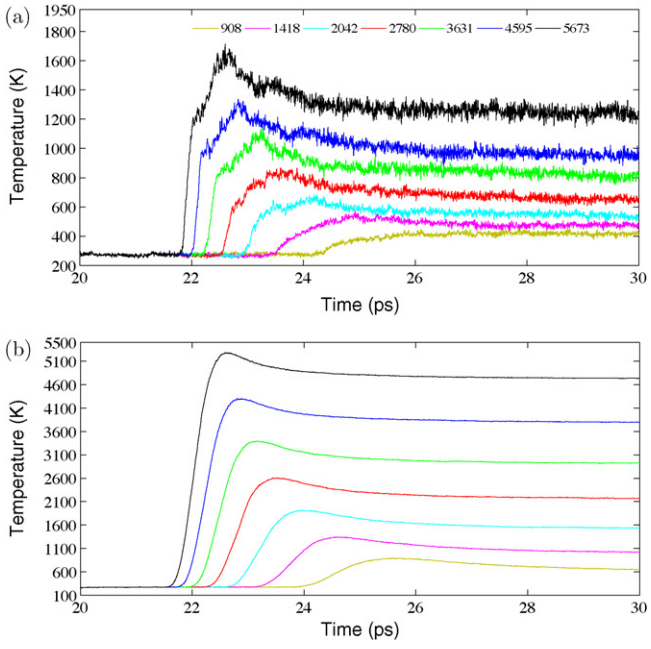

Fig. 3. Time evolution of the temperatures of echistatin (a) and water (b) at various impact energies (in eV). Water temperature is an average over all water molecules.

In our approach, we measure temperature as the total kinetic energy averaged over all water molecules (water temperature), or the entire protein (protein temperature). When converting energy to temperature, we take the fact into account that we consider H-atoms to be rigidly bonded; their vibrations thus do not contribute to the specific heat. After impact, the temperature steeply rises – for both the protein and the water – for all but the lowest impact energies. At later times, the temperature decreases again due to several effects: the (adiabatic) expansion of the system reduces temperature, as bonds are stretched and kinetic energy is converted to potential energy; water evaporates and takes energy out of the system; and – in the case of water – also the phase transition to the gas phase costs kinetic energy.

The water temperatures reached may appear excessively high. Consider, however, the case of $v = 2864$ m/s, which is the middle curve in Fig. 3. Each water molecule brings a kinetic energy of 0.77 eV with it when it impinges on the wall; equilibration among 6 degrees of freedom – we disregard vibrations involving H atoms in this study – gives a temperature of 3070 K, which is of the order of the maximum water temperature in Fig. 3. The temperature in the protein is, however, considerably lower; it does not surpass 850 K in this case. This smaller protein temperature is connected to the fact that the protein is protected during the droplet–wall collision by its hydration shell, and hence receives less direct impact energy. In addition, the water molecules which received the highest amount of energy in the collision process will leave the droplet earliest and take their high energy with them; this is the basis of the process of *evaporative cooling*. The protein cools more efficiently – for all but the lowest impact energy – than the water; the reason is that evaporating water molecules take energy away also from the protein. Even in the low-energy impact cases, where the protein remains hydrated, the temperatures of the protein and water are not equal; this is due to the fact that the water temperature has been determined as an average over all water molecules, including those that have evaporated from the droplet.

The collision process is accompanied by a strong loss of water molecules. The initial stage (in our case between 20 and 30 ps) has been termed the primary evaporation process [31]. Due to the high temperatures present after the collision evaporation proceeds as a slower but steady secondary evaporation process which we can follow until 150 ps.

In Fig. 4, we focus on the first hydration shell of the protein, which we define here as the water molecules within a distance of 3 Å from the protein. Note that during the impact itself the number of water molecules in the hydration shell seems to increase

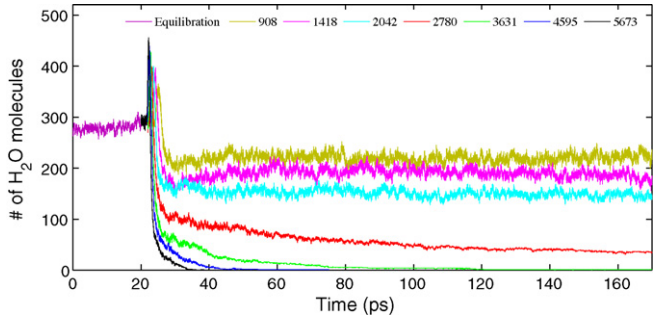

Fig. 4. Time evolution of the number of molecules in the first solvation shell (3 Å thickness) around the protein echistatin for various impact energies (in eV).

strongly; this is a consequence of the high pressure developing during the collision which pushes water molecules towards the protein. After the collision the hydration layer contains a smaller number of molecules for all impact energies studied, and this number decreases monotonically with impact energy. For the three smallest energies, the hydration shell appears to be stable after impact (apart from fluctuations). For the three highest impact energies, on the other side, the protein sheds off its entire hydration shell; so after a time varying between 20 and 120 ps in our simulations, the IDEM process results in a fully desolvated protein. The case of $v = 2864$ m/s is intermediate. As noted above this velocity corresponds to an energy of 0.77 eV/molecule, which is around 50% above the cohesive energy of water, 0.52 eV/molecule: Energy densities slightly above the cohesive energy of water are needed for fully desolvating the protein.

We thus conclude that impact energies of around 0.8–1 eV per water molecule are needed for producing protein which is completely free of water. Above this energy, desolvation proceeds quickly, within a few ten ps. We note, however, that the present force field may not be entirely accurate to predict the dynamics of the highly excited protein, as the temperatures to which the protein is heated here strongly surpass those at which these force fields are commonly used.

3.2. Secondary structure analysis

While mass spectrometry is mainly interested in isolating the protein and bringing it intact into the gas phase, we also study the conformational changes of the protein during this process. Even though these changes are of no direct experimental relevance, it is known that the desolvation process is influenced by (and influences itself) the protein conformation. In order to understand the structural changes of the protein during and after the collision, we perform a secondary structure analysis with the help of the STRIDE program [32] available within the Visual Molecular Dynamics (VMD) software package [33]. In this analysis, the aminoacids forming the linear protein backbone structure are enumerated (here from 1-49); each aminoacid is assigned the secondary structure type to which it belongs. In the initial 300-K equilibrium structure of echistatin in bulk water [Fig. 5(h)] 2 extended β-sheets are formed while the remaining aminoacids merely form turns or coils.

The changes in secondary structure after impact are presented in Fig. 5. Only little distortions of the protein conformation are found for the impact regime between 0.9 and 2.8 keV. However, severe distortions are found for the impact range of 3.6–5.7 keV. In detail, we find the following conformation changes. In the time period of 21–25 ps, the droplet–wall interaction induces structural changes which increase in strength with impact energy. For the case of 0.9–2.8 keV, the extended β-sheets are disrupted but recover until the end of the simulation. However, recovery does not take place in the case of 3.6–5.7 keV impact energy. Furthermore, we observe several transitions of coil, turn, and β-sheets into isolated bridge, 3-10 helix and vice versa. In most of the cases minor disruptions were observed. Interconversions of coil and turn are also found after the wall collision ($t > 30$ ps) until the end of the simulations. However, the overall stability of the secondary structure appears to be maintained; one may talk of a partially molten globular structure.

3.3. Root mean square deviation (RMSD)

The root mean square deviation is defined as the average deviation of the C_α atom positions in the protein from their positions in a reference structure. Here, we take the fully hydrated protein at 300 K as our reference. Thus the RMSD is a measure of the overall deviation from the reference backbone structure. Fig. 6 displays the time evolution of this quantity, while Table 1 assembles its average values over the period of time of 30–150 ps, i.e., in the after-collision regime. The RMSD is seen to rise sharply at the droplet–wall collision and to maintain its value thereafter, albeit with large fluctuations. While it increases strongly with impact energy, its increase is non-monotonic. However, it is possible to roughly divide the data into two groups. At small energies (0.9–2.8 keV), the RMSD is in the range of around 3–5 Å, while it increases beyond 6 Å for higher impact energies. The increase of the RMSD with impact energy is certainly due to the energization of the protein, as quantified by the protein temperature, Fig. 3(a). We note, however, that the strong increase for impact energies beyond 2.8 keV coincides with the complete shedding of the hydration layer, cf. Fig. 4. Also in other studies it has been found that the passage of the protein to the gas phase is commonly accompanied with major conformation changes [16,34,24].

3.4. Radius of gyration, R_{gyr}

The (mass-weighted) radius of gyration, R_{gyr}, is a measure of the compactness of a protein. It is defined as

$$R_{gyr} = \sqrt{\frac{\sum m_i \mathbf{r}_i^2}{\sum m_i}}, \tag{2}$$

where $\mathbf{r}_i$ is the distance of atom i from the centre of mass of the protein, and m_i its mass.

Table 1 shows that the equilibrium value of R_{gyr} in bulk water at ambient temperature is 11.24 Å. During the collision, R_{gyr} strongly increases, see Fig. 7; as the inset of this figure shows, the increase grows with the impact energy. This increase is due to the *lateral jetting* phenomenon described in Section 3.1 above and visualized in Fig. 1(b) and (c). When the liquid droplet splashes on the surface, the protein is spread out horizontally and follows the lateral motion of the water fluid. A closer analysis of the various Cartesian components of Eq. (2) shows that it is indeed the lateral components which contribute to the growth of R_{gyr} during collision.

After collision, R_{gyr} again shrinks and assumes a rather constant value. Note that the fluctuations after collision are considerably larger than before collision (Fig. 7); the size of the fluctuations increases with impact energy. This is a clear sign of the conformational fluctuations of the molecule, which were already visible in the secondary structure analysis, Fig. 5, and are caused by the increasingly high protein temperatures, Fig. 3(a).

The average values of R_{gyr} after collision (Table 1) appear to be mainly dependent on the amount of water remaining on the protein. For impact energies $E \leq 2.0$ keV, R_{gyr} returns roughly to

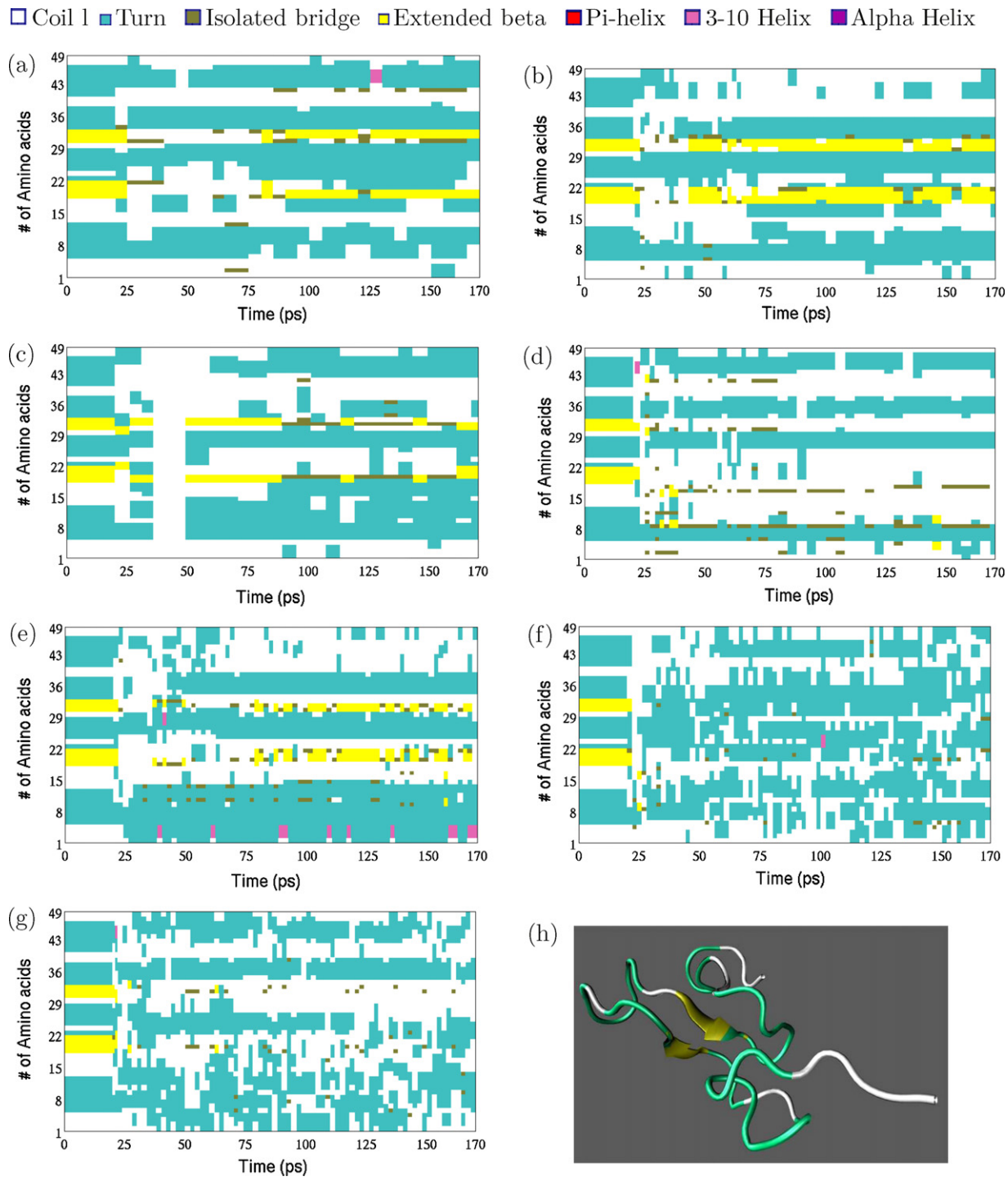

Fig. 5. Time evolution of the secondary structure of echistatin at various impact energies: (a) 908 eV, (b) 1418 eV, (c) 2042 eV, (d) 2780 eV, (e) 3631 eV, (f) 4595 eV and (g) 5673 eV. (h) Displays the conformation of echistatin in bulk water.

its bulk value; as shown in Fig. 4, these are the impact energies, where the first hydration shell survives the collision. For the two highest impact energies, $E \geq 4.6$ keV, however, the gyration radius has decreased. As here the protein has quickly got rid of all water molecules, it is free to assume a compact globular form. At the two intermediate energies of 2780 and 3631 eV, finally, we know from Fig. 4 that the hydration shell is severely damaged and decreases to less than 20% of the bulk value or entirely vanishes in the course of the simulation. In these cases a statistically significant increase of R_{gyr} is observed. We note that also in previous studies it was found that R_{gyr} increases both with temperature [35] and in a partial hydration state [15].

3.5. Solvent accessible and excluding surface area (SASA/SESA)

A further measure to quantify protein conformation changes is provided by the concepts of the solvent accessible surface area (SASA) and the solvent excluding surface area (SESA) [36–39]. These areas are meant to provide information about the hydrophilic (SASA) and hydrophobic (SESA) parts of the protein. Since the

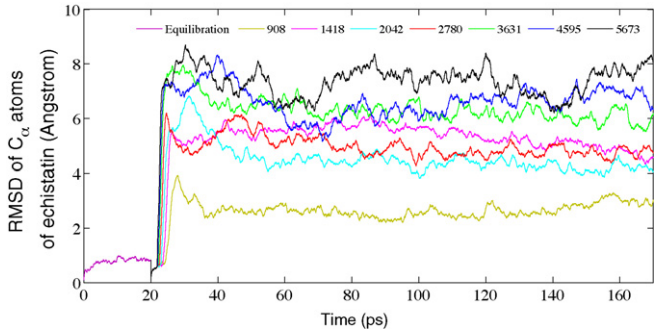

Fig. 6. Temporal evolution of the root-mean-square deviation (RMSD) of echistatin for various impact energies (in eV).

balance between the forces dominating protein–protein and protein–solvent interactions is crucial for establishing the secondary and the tertiary structure of proteins, these concepts are widely used in protein structural analysis. To measure SASA, a probe sphere is rolled over the van der Waals surface of the protein; SASA is the area traced out by the centre of the probe sphere during this motion. The radius of the probe sphere is taken as 1.4 Å, corresponding to the radius of a water molecule. SESA is the area of the corresponding surface which is not accessible to the probe sphere, due to steric hindrance by other parts of the protein. In the present work, we have calculated the SASA of the protein using the module developed by Lee and Richards [36] and implemented in CHARMM [12]. SESA was calculated as the difference between the SASA and the van der Waals surface area, cf., e.g., [16].

In bulk water, echistatin has a SASA of around 40 nm^2 and a SESA of around 8.8 nm^2, see Table 1 and Fig. 8, with moderate fluctuations. Upon collision with the wall, the SASA strongly increases, while the SESA almost vanishes. This is a sign of the strong collisional deformation of the molecule, which brings all parts of the protein in contact with the solvent. After the collisional phase, the surface areas return to about their initial values, but with a few notable changes: At small impact energies ($E \leq 2.0$ keV), the SASA stays above its original value, and the SESA below. At these energies, the hydration shell of the protein is still more or less intact, and influences the conformation of the hydrophobic and hydrophilic side chains of the protein. Due to the increased temperature of both protein and solvent and the conformational fluctuations of the protein, the SESA shrinks. The converse trend is seen for higher impact energies, $E \geq 2.8$ keV, where the SESA tends to assume larger, and the SASA smaller, values than in bulk water; we rationalize this behaviour by the fact that the protein has become depleted of the solvent or even free of it. As a consequence, the solvent is no longer important for determining the protein structure and the energetic cost for exposing the SESA has vanished.

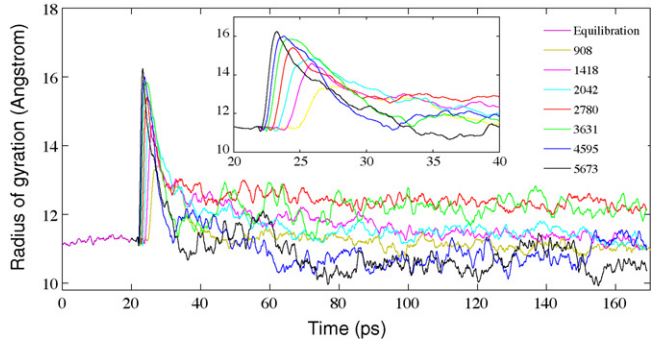

Fig. 7. Temporal evolution of the radius of gyration of echistatin for various impact energies (in eV).

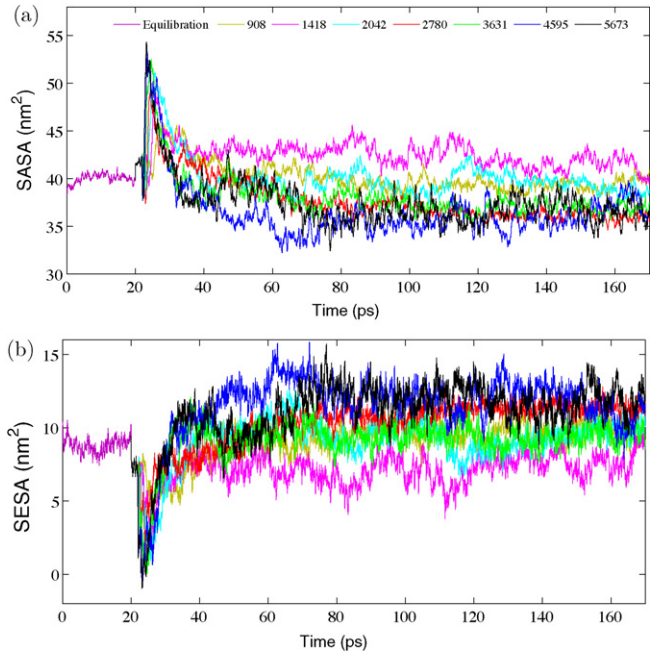

Fig. 8. Time evolution of solvent accessible surface area (a) and solvent excluding surface area (b) of echistatin for various impact energies (in eV).

3.6. Hydrogen bonds

We monitor the number of hydrogen bonds in our system in order to obtain information about the stability and restructuring of the hydrogen network. The number of hydrogen bonds between the protein and water molecules, HB_{ps}, and between different parts of the protein, HB_{pp}, are counted separately. In both cases, the H donor is a protein atom, typically a nitrogen atom. The H acceptor is an oxygen atom, which either is on the protein, typically in a C=O group, or belongs to a water molecule. We use a distance criterion ($r < 3.5$ Å) between donor and acceptor to identify a hydrogen bond [40,41]. For the hydrogen-donor–acceptor angle we accept a maximum angle of 30°, as in [16].

The time evolution of hydrogen bonds in our system is displayed in Fig. 9, while the average values are assembled in Table 1. We note that the bonds between the protein and water evolve in close analogy to the number of water molecules in the first hydration shell around the protein, Fig. 4. This is a plausible observation, since it means that water molecules take every chance to form a hydrogen bond with the protein. The number of intra-protein hydrogen bonds is more interesting. Upon collision, the strong protein deformation destroys around 50% of the bonds; however, these reform later. In addition, with increasing impact energy more and more intra-protein bonds form. It thus appears that the loss of protein–solvent bonds is compensated by the creation of new protein–protein bonds.

We quantify the total number of hydrogen bonds in Fig. 10. Here we normalize the data to the equilibrium values for echistatin in bulk water, $HB_{pp}^{equ} + HB_{ps}^{equ} = 393$, cf. Table 1:

$$HB = \frac{HB_{pp} + HB_{ps}}{HB_{pp}^{equ} + HB_{ps}^{equ}}. \quad (3)$$

The figure demonstrates that the protein attempts to keep the total number of hydrogen bonds constant; for every bond lost to a water molecule, the protein forms an intra-protein bond. Only for the 2 highest impact energies, the total number of bonds decreases slightly, by 14%; this is remarkably little in view of the fact that the system has lost 180 protein-water bonds.

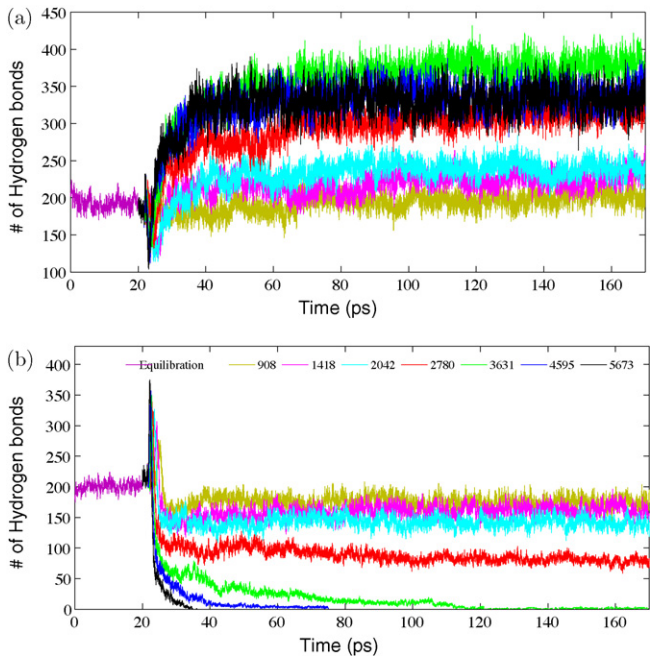

Fig. 9. Time evolution of the number of hydrogen bonds within the protein, HB_{pp}, (a) and between the protein and the water molecules, HB_{ps}, (b) for various impact energies (in eV).

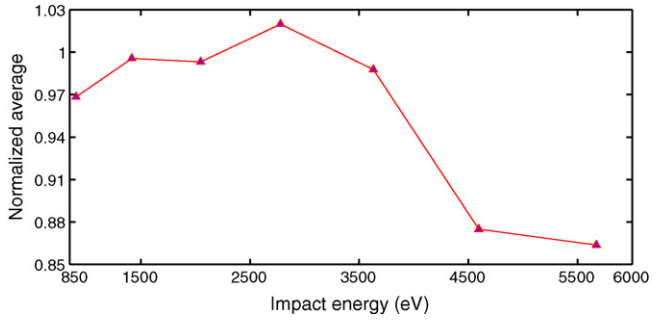

Fig. 10. Total number of hydrogen bonds of the protein, HB, Eq. (3), as function of impact energy. Data have been normalized to the equilibrium value in bulk water at 300 K, cf. Table 1. Lines are to guide the eye.

We conclude that the formation of intra-protein hydrogen bonds stabilizes the protein in its solvent-free vacuum phase and gives it a different conformation. Only for the highest impact energies – and consequently protein temperatures – become these hydrogen bonds somewhat destabilized.

4. Conclusions

We have investigated the IDEM process using molecular dynamics simulation for a specific protein (echistatin). For a series of impact energies, we have studied the protein denaturation and conformation stability by measuring the radius of gyration, the root mean squared deviation, and the solvent accessible and excluding surface areas. Furthermore we monitor the changes in the secondary structure using the STRIDE programme and the evolution of the hydrogen bonds between protein and solvent and within the protein. Our main findings concern the velocity dependence of the protein dehydration process:

1. The energy transfer to the water droplet, and then to the protein, occurs fast, within a few ps. The temperatures of water and of the protein increase monotonically with impact energies.
2. The resulting dehydration process of the protein occurs on a longer time scale spanning at least tens of ps, and depends sensitively on the collision speed.
3. Impact energies slightly (in our case: 50%) above the cohesive energy of water are needed for fully desolvating the protein.

Our structural analysis of the protein after the impact shows that the minimum thickness of the water which is needed to preserve the non-denatured conformation of the protein, one monolayer of water, can be realized by carefully tuning the impact velocity. At the lowest impact velocities of 1.6–2.9 km/s the protein is at the end of the simulation still covered by a water hydration shell. The conformational distortions are small and do not affect the secondary structure. By carefully choosing the impact velocity (2.0 km/s in our study), it is possible to obtain a protein which has shed off the water hydration layer most gently, and retained its secondary structure almost intact. At the highest impact velocities (3.7–4.1 km/s) we find solvent-free intact protein. The secondary structure and the hydrogen bonding suggest that the protein is strongly distorted. Due to the entire loss of the hydration shell, the protein forms a large compensating number of intra-protein hydrogen bonds.

A number of questions remain open which need be addressed in future studies. Most importantly, a protein model which allows bond breaking will be essential in order to study the question under which conditions fragmentation of the protein will occur. In our study the high protein temperature only became apparent in denaturation of its conformation and a high vibrational activity, which shows up particularly in the low-frequency so-called *conformational* modes. While the covalent bond energy is considerably larger than the energetic equivalent of the temperatures found in our study, thermal fluctuations may put sufficient energy into a single bond to break it. Thus it will be interesting to study the fate of partially hydrated proteins on longer time scales, in order to assess the long-term evaporation and also protein stability against fragmentation. The time scales of interest to experiment (in the order of μs) are not directly accessible to molecular dynamics, such that either hybrid simulation schemes or analytical tools of statistical mechanics must be used.

Acknowledgments

The authors acknowledge financial support by the Deutsche Forschungsgemeinschaft via the Graduiertenkolleg 792.

Appendix A. Supplementary data

Supplementary data associated with this article can be found, in the online version, at doi:10.1016/j.ijms.2009.10.002.

References

[1] S.A. Aksyonov, P. Williams, Rap. Commun. Mass Spectrom. 15 (2001) 2001.
[2] J.F. Mahoney, J. Perel, S.A. Ruatta, P.A. Martino, S. Husain, K. Cook, T.D. Lee, Rapid Commun. Mass Spectrom. 5 (1991) 441.
[3] W. Christen, U. Even, Eur. Phys. J. D 9 (1999) 29.
[4] I. Schek, T. Raz, R.D. Levine, J. Jortner, J. Chem. Phys. 101 (1994) 8596.
[5] W. Christen, Int. J. Mass Spectrom. Ion Proc. 174 (1998) 35.
[6] S. Zimmermann, H.M. Urbassek, Eur. Phys. J. D 39 (2006) 423.
[7] S. Zimmermann, H.M. Urbassek, Phys. Rev. A 74 (2006) 063203.
[8] B. Wyatt, Comput. Math. Appl. 28 (1994) 175.
[9] M. Svanberg, L. Ming, N. Marković, J.B.C. Pettersson, J. Chem. Phys. 108 (1998) 5888.
[10] J. Eggers, J.R. Lister, H.A. Stone, J. Fluid Mech. 401 (1999) 293.
[11] H.A. Stone, Annu. Rev. Fluid Mech. 26 (1994) 65.
[12] M.F. Jarrold, Annu. Rev. Phys. Chem. 51 (2000) 179.
[13] S. Melchionna, G. Briganti, P. Londei, P. Cammarano, Phys. Rev. Lett. 92 (2004) 58101.
[14] O.O. Sogbein, D.A. Simmons, L. Konermann, J. Am. Soc. Mass Spectrom. 11 (2000) 312.
[15] M. Sadeghi, X. Wu, A. Vertes, J. Phys. Chem. B 105 (2001) 2578.

[16] A. Patriksson, E. Marklund, D. van der Spoel, Biochemistry 46 (2007) 933.
[17] J.B. Fenn, M. Mann, C.K. Meng, S.F. Wong, C.M. Whitehouse, Science 246 (1989) 64.
[18] R. Hartman, D. Brunner, D. Camelot, J. Marijnissen, B. Scarlett, J. Aerosol Sci. 31 (2000) 65.
[19] J.M. Lopez-Herrera, A.M. Ganan-Calvo, J. Fluid Mech. 501 (2004) 303.
[20] L. Konermann, J. Phys. Chem. B 111 (2007) 6534.
[21] M. Nakamura, A. Takamizawa, H. Yamada, K. Hiraoka, S. Akashi, Rapid Commun. Mass Spectrom. 21 (2007) 1635.
[22] A.A. Rostom, C.V. Robinson, J. Am. Chem. Soc. 121 (1999) 4718.
[23] Y. Mao, J. Woenckhaus, J. Kolafa, M.A. Ratner, M.F. Jarrold, J. Am. Chem. Soc. 121 (1999) 2712.
[24] P.J. Steinbach, B.R. Brooks, Proc. Natl. Acad. Sci. U.S.A. 90 (1993) 9135.
[25] M.F. Jarrold, Phys. Chem. Chem. Phys. 9 (2007) 1659.
[26] B.R.R. Brooks, C.L.L. Brooks, A.D.D. Mackerell, L. Nilsson, R.J.J. Petrella, B. Roux, Y. Won, G. Archontis, C. Bartels, S. Boresch, et al., J. Comput. Chem. 30 (2009) 1545.
[27] Y. Dou, N. Winograd, B.J. Garrison, L.V. Zhigilei, J. Phys. Chem. B 107 (2003) 2362.
[28] X. Wu, M. Sadeghi, A. Vertes, J. Phys. Chem. B 102 (1998) 4770.
[29] W.L. Jorgensen, J. Chandrasekhar, J.D. Madura, R.W. Impey, M.L. Klein, J. Chem. Phys. 79 (1983) 926.
[30] J.-P. Ryckaert, G. Ciccotti, H.J.C. Berendsen, J. Comput. Phys. 23 (1977) 327.
[31] M.B. Hamaneh, M. Buck, Biophys. J. 92 (2007) L49.
[32] D. Frishman, P. Argos, Proteins Struct. Funct. Genet. 23 (1995) 566.
[33] W. Humphrey, A. Dalke, K. Schulten, J. Mol. Graph. 14 (1996) 33.
[34] A. Caflisch, M. Karplus, Proc. Natl. Acad. Sci. U.S.A. 91 (1994) 1746.
[35] O. Guvench, C.L. Brooks, J. Comput. Chem. 25 (2004) 1005.
[36] B. Lee, F.M. Richards, J. Mol. Biol. 55 (1971) 379.
[37] F.M. Richards, Ann. Rev. Biophys. Bioeng. 6 (1977) 151.
[38] A.R. Bizzarri, S. Cannistraro, J. Phys. Chem. B 106 (2002) 6617.
[39] J.L. Pascual-Ahuir, E. Silla, I. Tunon, J. Mol. Struct. (Theochem) 426 (1998) 331.
[40] H. De Loof, L. Nilsson, R. Rigler, J. Am. Chem. Soc. 114 (1992) 4028.
[41] A.V. Morozov, T. Kortemme, K. Tsemekhman, D. Baker, Proc. Natl. Acad. Sci. U.S.A. 101 (2004) 6946.